International Geology Review
Publication details, including instructions for authors and subscription information:
http://www.informaworld.com/smpp/title~content=t902953900

Emplacement age of the Songshugou ultramafic massif in the Qinling orogenic belt, and geologic implications

Junfeng Liu [ab]; Yong Sun [b]; Laixi Tong [a];Weidong Sun [ac]
[a] CAS Key Laboratory of Isotope Geochronology and Geochemistry, Guangzhou Institute of Geochemistry, Chinese Academy of Sciences, China [b] The State Key Laboratory of Continental Dynamics, Department of Geology, Northwest University, Xi'an, China [c] School of Earth and Space Sciences, University of Science and Technology of China, Hefei, China

To cite this Article Liu, Junfeng , Sun, Yong , Tong, Laixi andSun, Weidong(2009) 'Emplacement age of the Songshugou ultramafic massif in the Qinling orogenic belt, and geologic implications', International Geology Review, 51: 1, 58 — 76
To link to this Article: DOI: 10.1080/00206810802650576
URL: http://dx.doi.org/10.1080/00206810802650576

International Geology Review
Vol. 51, No. 1, January 2009, 58–76

Emplacement age of the Songshugou ultramafic massif in the Qinling orogenic belt, and geologic implications

Junfeng Liu[a,b], Yong Sun[b], Laixi Tong[a] and Weidong Sun[a,c]*

[a]*CAS Key Laboratory of Isotope Geochronology and Geochemistry, Guangzhou Institute of Geochemistry, Chinese Academy of Sciences, China;* [b]*The State Key Laboratory of Continental Dynamics, Department of Geology, Northwest University, Xi'an, China;* [c]*School of Earth and Space Sciences, University of Science and Technology of China, Hefei, China*

(*Accepted 27 October 2008*)

The Songshugou ultramafic massif is located to the north of the Shang-Dan fault, the Palaeozoic suture between the North and South China blocks. It is the largest Apline-type ultramafic body in the Qinling orogenic belt of central China, consisting mainly of dunite with a small amount of harzburgite and minor pyroxenite. We present new LA-ICP-MS U−Pb dating and trace element results for zircon from two garnet amphibolite samples in the contact metamorphic zone surrounding the massif. One was sampled ~1 m from the massif, the other ~5 m away. The studied zircon grains are small, anhedral, and display typical metamorphic characteristics of low Th/U values (<0.1). The U and Th concentrations of zircon range from several hundred ppm to less than 10 ppm. Cathodoluminescence images show two apparent generations of zircon, with lighter cores and darker rims. Core and rim ages however, are identical within error. These two samples yield identical concordant ages of 506 ± 7 and 510 ± 7 Ma, suggesting that the Songshugou ultramafic massif was emplaced at ~510 Ma. Low HREE concentrations and the absence of Eu anomalies in most analysed zircons suggest that the studied grains most likely formed during garnet amphibolite metamorphism induced by emplacement of the ultramafic massif.

To better understand the cooling history of the massif, $^{40}Ar/^{39}Ar$ ages of amphibole from three garnet amphibolite specimens in the contact metamorphic zone and one amphobolite sample about 20 m away from the massif were determined. The $^{40}Ar/^{39}Ar$ ages increase from 372 ± 15 Ma (JSM-01) near the massif to disturbed, unreliable 'plateau' ages of 474 ± 8 Ma (JSM-03) and 781 ± 146 Ma (JSM-04) with increasing distance from the ultramafic massif, showing limited heating during exhumation of the massif, followed by slow cooling. Therefore, the Songshugou ultramafic massif does not reflect the Jining orogeny at ~1 Ga. Instead, it was emplaced into the Proterozoic, Qinling Group during the Palaeozoic, probably due to the subduction along the Shang-Dan fault.

Keywords: Qinling orogenic belt; Songshugou; ultramafic massif; zircon dating; laser ablation

*Corresponding author. Email: weidongsun@gig.ac.cn

ISSN 00200-6814 print/ISSN 1938-2839 online

DOI: 10.1080/00206810802650576
http://www.informaworld.com

Introduction

The Qinling orogenic belt in central China is the middle-western part of the suture between the North and South China blocks (Zhang *et al.* 1995a,b; Zhang 1997; Meng and Zhang 1999; Sun *et al.* 2002b). It is of critical importance for understanding the interaction between these two blocks and the tectonic evolution of China (Mattauer *et al.* 1985; Zhang *et al.* 1989, 2004; Lerch 1993; Lerch *et al.* 1995; Gilder and Courtillot 1997; Meng and Zhang 1999, 2000).

There are over 100 ultramafic massif bodies, widely distributed along the Qinling Mountains. These massifs are generally closely related to the evolution of the Qinling orogenic belt. One of them, the Songshugou ultramafic massif, is the largest Alpine-type ultramafic body in China (Huang 1984; Li *et al.* 1991; Zhang 1993; Sun *et al.* 1997), covering an area of ~20 km^2. Remarkably, the Songshugou ultramafic massif consists mainly of dunite (~90%), with a small amount of harzburgite and minor pyroxenite (Liu *et al.* 1995).

The Songshugou massif has gained wide interest since the 1950s, because of its unique characteristics and important tectonic settings, which are very important for understanding the history of the Qinling orogenic belt and the interaction between the North and South China blocks. It is, however, still controversial as to how it formed and when it emplaced into the Proterozoic Qinling Group (An *et al.* 1981; Wang *et al.* 1982, 2005; Huang 1984; Xu *et al.* 1988; Gao 1990; Li *et al.* 1991; Liu *et al.* 1995, 2004; Dong *et al.* 1997; Zhang *et al.* 2001; Su 2004). For example, based on studies of structure and strata, the Songshugou massif was initially interpreted as magmatic fractionation at high temperature, which then erupted (Northwest Metallurgy 713 Team 1961), similar to komatiite. Later on, it was considered to be a residual of mantle melting, which intruded into the Qinling Group at low temperature through complicated tectonic processes associated with an intense metamorphic event in the Late Precambrian (650~830 Ma) in the Songshugou region (An *et al.* 1981). Furthermore, the ultramafic massif might have suffered high-temperature and low-temperature metamorphisms (Xu *et al.* 1988). Others proposed that the emplacement time of the massif was Neoproterozoic (Li *et al.* 1991; Liu *et al.* 2004). These ages were taken as evidence of major Jinning tectonic movement (~1.0 Ga) in the Qinling orogenic belt. Given that the Songshugou massif has been regarded as part of an ophiolite, it was further speculated that there was a Proterozoic oceanic basin in the region (B. Zhang *et al.* 1998; G. Zhang *et al.* 2001). Others suggested that the Songshugou massif was part of the Neoproterozoic super plume, which formed during the same event as other Neoproterozoic mafic and ultramafic rocks widely distributed in South China Block (Su 2004), e.g. mafic dikes in the South China (Z.X. Li *et al.* 2003; W.X. Li *et al.* 2005; Li *et al.* 2005a), and Jinchuan to the west of Qinling (Li *et al.* 2005b). Namely, the Songshugou ultramafic rocks, together with nearby Hannan mafic-ultramafic intrusions, were associated with a mantle plume (Su *et al.* 2005).

The emplacement age of the Songshugou massif is one of the keys for understanding its evolution and geological significance with respect to the evolution of the whole Qinling orogenic belt. In this study, we analysed the U–Pb ages and trace elements of zircon from garnet amphibolite in the contact metamorphic zone using LA-ICP-MS methods. In addition, four amphibole samples collected across the contact metamorphic zone were dated using $^{40}Ar/^{39}Ar$ methods. Our results show that the Songshugou massif was emplaced into the Qinling group at ~510 Ma, and cooled down slowly for more than 100 Myr.

Geological setting

The Qinling orogenic belt can be divided into four zones, known as the South margin of the North China Block, the North Qinling zone, the South Qinling zone, and the North margin of the Yangtze Block, which are separated by the Luonan-Luanchuan, Shang-Dan, and Mian-Lue faults, respectively (Zhang *et al.* 1989) (Figure 1). The north Qinling zone is regarded as the North Qinling arc system, separated from the south margin of the NCB by a backarc basin (Xue *et al.* 1996; Sun 2002b). It consists of strongly deformed metasediments and metavolcanic rocks, including Qinling (Pt_1), Kuanping ($Pt_{2\text{-}3}$), Erlangping, and Danfeng Groups. These sediments were deposited in continental shelf and slope environments from the Late Proterozoic to the Early Palaeozoic. The volcanic rocks typically show geochemical characteristics of continental tholeiites and were probably erupted in a rift setting (Wang *et al.* 1991; Lerch 1993) at ~1.0 Ga (Zhang 1991).

The Songshugou ultramafic massif belongs to the North Qinling zone, which is located to the north of the Shang-Dan fault in Shangnan County, Shaanxi Province. It consists predominantly of fine-grained dunite (~90%), with minor harzburgite, coarse-grained dunite, tilaite and thin veins of pyroxenite. Dunite distributes mainly in the centre, whereas other rocks scatter more in the margin. The ultramafic rocks are fairly fresh, with a thin serpentinized rim surrounding the massif. Observation under the microscope shows penetrative schistosity, whereas fine-grained dunite has already changed to mylonite as a result of multiple deformation (Liu *et al.* 2004). Medium- to coarse-grained dunite occurs as lenses of different sizes in fine-grained dunite mylonite. Harzburgite and tilaite appear as segregation in dunite layers.

The Songshugou ultramafic massif intruded into the Proterozoic Qinling Group (Figure 1). Surrounding the massif, there is a garnet amphibolite 'coating' ~2−10 m thick, which was formed during thermal contact metamorphism, most likely related to the emplacement of the massif. These together are surrounded by marble and felsic gneiss of the Qinling Group (Figure 2).

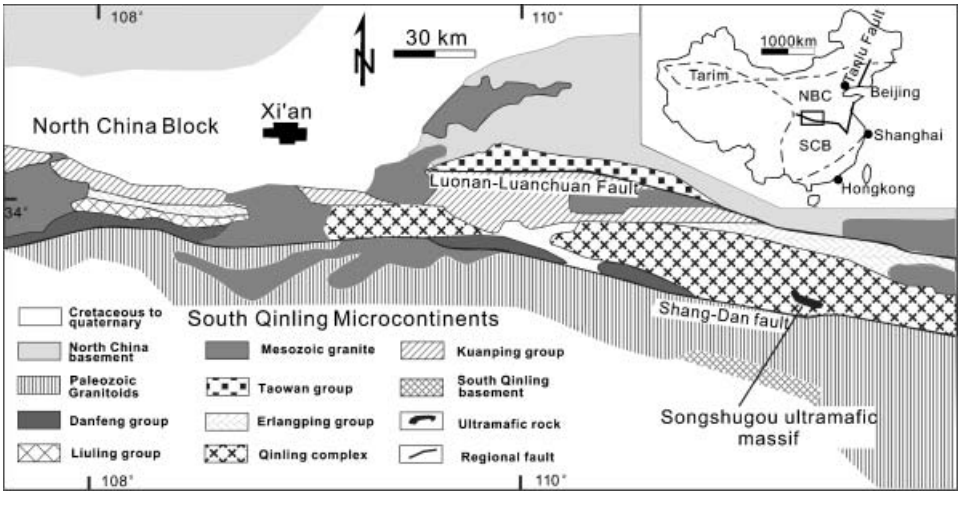

Figure 1. Geological sketch map of the Qinling Mountains (compiled from Xue *et al.* 1996; Zhang *et al.*, 2001 and Sun *et al.* 2002).

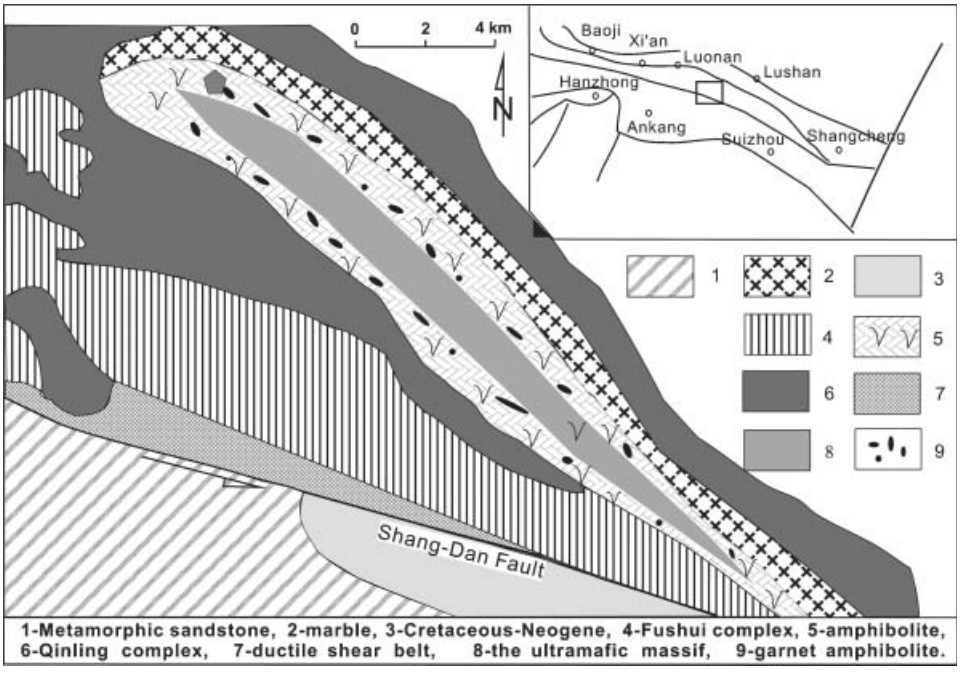

Figure 2. Distribution of the Songshugou ultramafic massif and position of sampling.

The contact metamorphic zone consists mostly of garnet amphibolite, which changes gradually to regional metamorphosed amphibolite outward (the wall rock). It locally intercalated with minor lenticular marble. The garnet amphibolite is mainly composed of garnet (>30%) and amphibole. Garnet commonly shows nubbly structure, occurring as lenses in the amphibolite. Relics of high-pressure granulite or garnet clinopyroxenite, overprinted by the amphibolite facies, have been reported in the contact metamorphic zone (Liu and Zhou 1994; Liu *et al.* 1995). Garnet with nubbly structures is usually surrounded by plagioclase, which is retrograde metamorphic product of garnet.

The amphibolite consists of plagioclase, hornblende, silicate and quartz, etc. Published data suggested that the protolith of the amphibolite wall rock was metamorphic mafic volcanic rocks (Zhou *et al.* 1995; Pei *et al.* 1996; Zhang *et al.* 2001), with trace element characteristics ranging from N-MORB to E-MORB types (Liu *et al.* 2004).

Samples and methods

In this study, we selected two fresh garnet amphibolite samples from the contact metamorphic zone, S-02 and S-06, for LA-ICP-MS U−Pb zircon dating. Sampling locations (N33°35′958″, E110°57′601″) are shown in Figure 2. Samples were first crushed through a mechanical corundum disintegrator ST-4 (Wuhan, China) to ~200 μm in diameter, followed by separation using conventional heavy liquid and magnetic techniques. Finally, zircon grains were hand-picked under a binocular microscope and then mounted in epoxy resin and polished down to half to expose the grain centres. The selection of zircon for isotopic analyses was done on the basis of cathodeluminescence (CL) images (Figure 3). CL imagines were taken using an

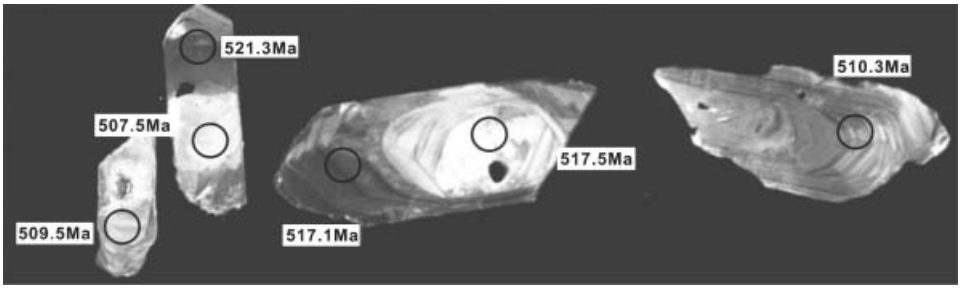

Figure 3. Representative CL images for zircon from the garnet amphibolite in the contact metamorphic zone.

electron microprobe (JEOLJXA-8800M) at the Electron Microprobe Lab, Beijing Institute of Geology and Geophysics, the Chinese Academy of Sciences. Most of the selected zircon grains are small ($60-130\,\mu$m in length, $30-70\,\mu$m in width), anhedral, transparent or tinctorial, with two generations, lighter cores and darker rims.

U–Pb zircon dating was carried out at the State Key Laboratory of Continental Dynamics, Northwest University, China (Liu and Sun 2005). Both an ELAN6100DRC from Perkin-Elmer/SCIEX (Ont., Canada) with a dynamic reaction cell (DRC) and, later on an Agilent 7500a were used. A Geolas 200M laser-ablation system was used for laser-ablation experiments. The system is equipped with a 193 nm Lambda Physik ArF-excimer laser and an imaging optical system designed by Güenther (1997). A spot diameter of 30 μm was applied to all analyses. Isotopes analysed for dating were: ^{29}Si, ^{206}Pb, ^{207}Pb, ^{208}Pb, ^{235}U, ^{238}U and ^{232}Th. Analytical processes are similar to those described by previous authors (Liu *et al.* 2002; Yuan *et al.* 2003).

A zircon standard (Harvard 91500) was used as an external standard for age calculation, and a glass standard (NIST 610) as the external standard for the concentration calculation. A minor isotope of Si (^{29}Si) was used as an internal standard. The SiO_2 content in zircon is assumed to be 32.78% for all samples. The international zircon standard, TEM, was analysed to test the reliability of the results. The weighted average ^{206}Pb/^{238}U age of TEMORA analyses during our study was 417 ± 1 Ma, which is consistent with the recommended value of 416.75 ± 0.24 Ma, within error (Black 2003).

Isotopic ratios and U, Th and Pb concentrations were calculated using GLITER 4.0, whereas ages were calculated using Isoplot program (ver. 2.49). Concentration values of NIST SRM 610 used for the external calibration are taken from (Pearce *et al.* 1997). The age of the 91500 used for calculation was 1064 Ma (Wiedenbeck *et al.* 1995).

To better constrain the geological meaning of zircon ages, we also analysed trace elements near some of the spots for age determination. Isotopes analysed for trace elements analyses were: ^{31}P, ^{42}Ca, ^{45}Sc ^{89}Y, ^{139}La, ^{140}Ce, ^{141}Pr, ^{143}Nd, ^{147}Sm, ^{151}Eu, ^{157}Gd, ^{159}Tb, ^{163}Dy, ^{165}Ho, ^{166}Er, ^{169}Tm, ^{173}Yb, ^{175}Lu, ^{208}Pb, ^{232}Th, and ^{238}U. NIST SRM 610 was used as the external standard for the concentration calculation (Pearce *et al.* 1997). Concentrations were calculated by using GLITER 4.0.

Four samples (JSM-01, JSM-02, JSM-03, JSM-04) across the contact metamorphic zone with intervals of 2–3 m from inside outward were selected for ^{40}Ar/^{39}Ar dating. Sampling locations are close to those for zircon dating

(N33°35′958″, E110°57′601″). JSM-01, JSM-02, JSM-03 are garnet amphibolite samples in the contact metamorphic zone. JSM-04 is a wallrock amphibolite, which was not obviously affected by the contact metamorphism. Amphibole separates were collected using conventional methods for laser heating $^{40}Ar/^{39}Ar$ dating. About 100 amphibole grains ~1 mm in diameter were picked for each analysis. All the samples were neutron irradiated together with standards in No. 49-2 nucleus reactor at the Institute of High Energy Physics, the Chinese Academy of Sciences. Instantaneous flux of the neutron is $6.0 \times 10^{12} - 6.5 \times 10^{12}$ (n/cm^2·s). Argon isotope analyses were carried out at the Key Laboratory of Isotope Geochronology and Geochemistry, Guangzhou Institute of Geochemistry, the Chinese Academy of Sciences, using GV5400 Ar rare gas MS. The results were calculated and plotted by using ArArCALC (2.1) (Koppers 2002). Detailed technology and processes are similar to those in the literature (Onstotta *et al.* 1991; Qiu and Wijbrans 2006).

Analytical results

U–Pb dating

Fifteen and eleven U/Pb dating analyses were obtained for sample S-02 and S-06, respectively. The values of ^{206}Pb, ^{207}Pb, ^{208}Pb, ^{235}U, ^{238}U and ^{232}Th were corrected using the program of Andersen (2002). The detailed results are listed in Table 1. All analyses are concordant and yield weighted average $^{206}Pb/^{238}U$ ages of 506.2 ± 7.4 Ma for S-02, and 510.4 ± 7.5 Ma for S-06 (Figure 4), which are consistent with each other within error.

Trace element

The trace element results of zircon samples (Figure 5) are presented in Table 2. All analyses were carried out near the age spots. Most zircon grains have consistent REE patterns with flat HREE and no obvious Eu negative anomaly. The REE pattern of spot LJF-1.03 is distinctively different from other zircon grains. It has considerably higher REE concentrations and obvious Eu negative anomaly.

The Th/U ratios of zircon from these two samples are mostly less than 0.1, with a few exceptions. Therefore, most of the zircon grains are metamorphic in origin, such that the ages represent a metamorphic event. Zircon domains with Th/U higher than 0.1 are usually very small (less than 30 μm), possibly due to inherited magmatic zircon.

$^{40}Ar/^{39}Ar$ dating

Amphiboles $^{40}Ar/^{39}Ar$ dating results of garnet amphibolite and amphibolite are shown in Figure 6 and Table 3. Two of the samples that were collected close to the ultramafic massif (JSM-01, JSM-02) yielding plateau ages of 372 ± 15 Ma (JSM-01), 464 ± 12 Ma (JSM-02), respectively. The other two samples away from the ultramafic body yield disturbed plateau ages of 474 ± 8 Ma (JSM-03), 781 ± 146 Ma (JSM-04). No reliable isochron ages were obtained.

Discussion

Emplacement of Songshugou massif

The average age of zircon from the Songshugou contact metamorphic zone (~510 Ma) is significantly younger than previous results (~980 Ma), which were used to

Table 1. U–Th–Pb LA-ICP-MS data for garnet amphibolite sample S-02 and S-06 in the contact metamorphic zone.

Spot	Content				U-Th-Pb isotopic ratios						Ages(Ma)					
S-02	Th (ppm)	U (ppm)	Pb* (ppm)	Th/U	Pb^{207}/Pb^{206}	1σ	Pb^{207}/U^{235}	1σ	Pb^{206}/U^{238}	1σ	Pb^{207}/Pb^{206}	1σ	Pb^{207}/U^{235}	1σ	Pb^{206}/U^{238}	1σ
Sep01d05	0.446	11.2	1.04	0.03	0.08004	0.0133	0.90381	0.14632	0.0819	0.00344	1198	296.89	653.8	78.04	507.5	20.47
Sep01d06	0.0191	4.24	0.391	0.004	0.06476	0.01929	0.75197	0.22002	0.08422	0.00512	766.6	526.96	569.4	127.52	521.3	30.42
Sep01d09	0.927	21.2	2.01	0.04	0.05798	0.00757	0.65691	0.08399	0.08217	0.0025	528.8	263.48	512.7	51.47	509.1	14.92
Sep01d11	0.509	9.16	0.757	0.05	0.07324	0.00994	0.81497	0.10802	0.08071	0.00264	1020.7	252.75	605.2	60.43	500.4	15.76
Sep01d12	0.245	7.85	0.722	0.03	0.2086	0.01893	2.36849	0.19899	0.08236	0.00317	2894.7	140.09	1233.1	59.98	510.2	18.86
Sep01d13	0.609	14.3	1.28	0.04	0.06809	0.00804	0.76219	0.08773	0.08119	0.00242	871.4	227.07	575.3	50.55	503.2	14.43
Sep01d14	1.91	28.5	2.37	0.06	0.07052	0.00399	0.7883	0.04349	0.08109	0.00137	943.4	111.64	590.2	24.7	502.6	8.18
Sep01d18	0.0503	9.73	1.14	0.005	0.10476	0.01375	1.19837	0.15155	0.08297	0.00327	1710.2	223.77	799.8	70	513.8	19.46
Sep01d19	0.0835	3.67	0.357	0.02	0.06784	0.0293	0.78113	0.33165	0.08352	0.00723	863.8	706.22	586.1	189.07	517.1	43
Sep01d20	0.137	5.55	0.547	0.02	0.0913	0.02298	1.05201	0.25614	0.08358	0.00588	1452.7	415.87	729.9	126.74	517.5	34.95
Sep01d22	0.523	30.8	2.62	0.01	0.05436	0.00324	0.61592	0.03597	0.08219	0.00135	385.8	128.43	487.3	22.6	509.2	8.01
Sep01d23	0.016	3.03	0.223	0.005	0.06198	0.03349	0.68882	0.36901	0.08061	0.00621	673.5	863.96	532.1	221.86	499.8	37.04
Sep01d24	1.081	19.4	1.68	0.05	0.0663	0.00606	0.7447	0.06638	0.08147	0.00195	816	180.2	565.1	38.63	504.9	11.64
Sep01d26	0.441	8.42	0.739	0.05	0.06576	0.01207	0.73979	0.13248	0.08159	0.00363	798.8	343.73	562.3	77.32	505.6	21.64
Sep01d27	0.217	16.1	1.52	0.01	0.11716	0.00905	1.31179	0.09654	0.08121	0.00222	1913.3	132.56	850.9	42.4	503.4	13.25
S-06																
Sep01e04	0.455	12.3	1.04	0.03	0.0547	0.0066	0.62119	0.07366	0.08237	0.00216	400.1	249.8	490.6	46.13	510.3	12.89
Sep01e07	1.23	12.2	1.12	0.1	0.09769	0.0114	1.11833	0.12555	0.08303	0.003	1580.4	203.81	762.2	60.18	514.2	17.88
Sep01e08	1.58	16.5	1.58	0.095	0.10239	0.00749	1.15283	0.08103	0.08166	0.00197	1667.8	129.48	778.6	38.22	506.1	11.72
Sep01e11	0.0182	2.4	0.196	0.007	0.10409	0.0344	1.16662	0.37502	0.08128	0.00677	1698.4	510.04	785.1	175.75	503.8	40.35
Sep01e12	0.424	13.3	1.40	0.03	0.14894	0.01273	1.73233	0.13995	0.08435	0.0027	2333.7	139.46	1020.6	52.01	522.1	16.05
Sep01e13	0.22	13.1	1.18	0.01	0.07004	0.0095	0.80519	0.10642	0.08337	0.00286	929.6	255.99	599.8	59.86	516.2	17.04
Sep01e14	7.83	41.4	3.77	0.18	0.07458	0.00375	0.84462	0.0413	0.08213	0.00134	1056.9	98.43	621.7	22.73	508.8	8
Sep01e16	2.84	20.1	1.85	0.14	0.1016	0.00603	1.11733	0.06375	0.07976	0.00163	1653.5	106.2	761.7	30.57	494.7	9.76
Sep01e17	0.770	12.3	1.13	0.06	0.03613	0.01055	0.41301	0.12001	0.0829	0.00281	0.1	32.63	351	86.24	513.4	16.71
Sep01e18	27.4	76.6	8.53	0.35	0.1054	0.00712	1.22939	0.07948	0.08458	0.00199	1721.3	119.14	814.1	36.2	523.4	11.8
Sep01e19	7.70	44.9	4.45	0.17	0.11765	0.00831	1.35722	0.09136	0.08365	0.00212	1920.9	121.5	870.7	39.35	517.9	12.62

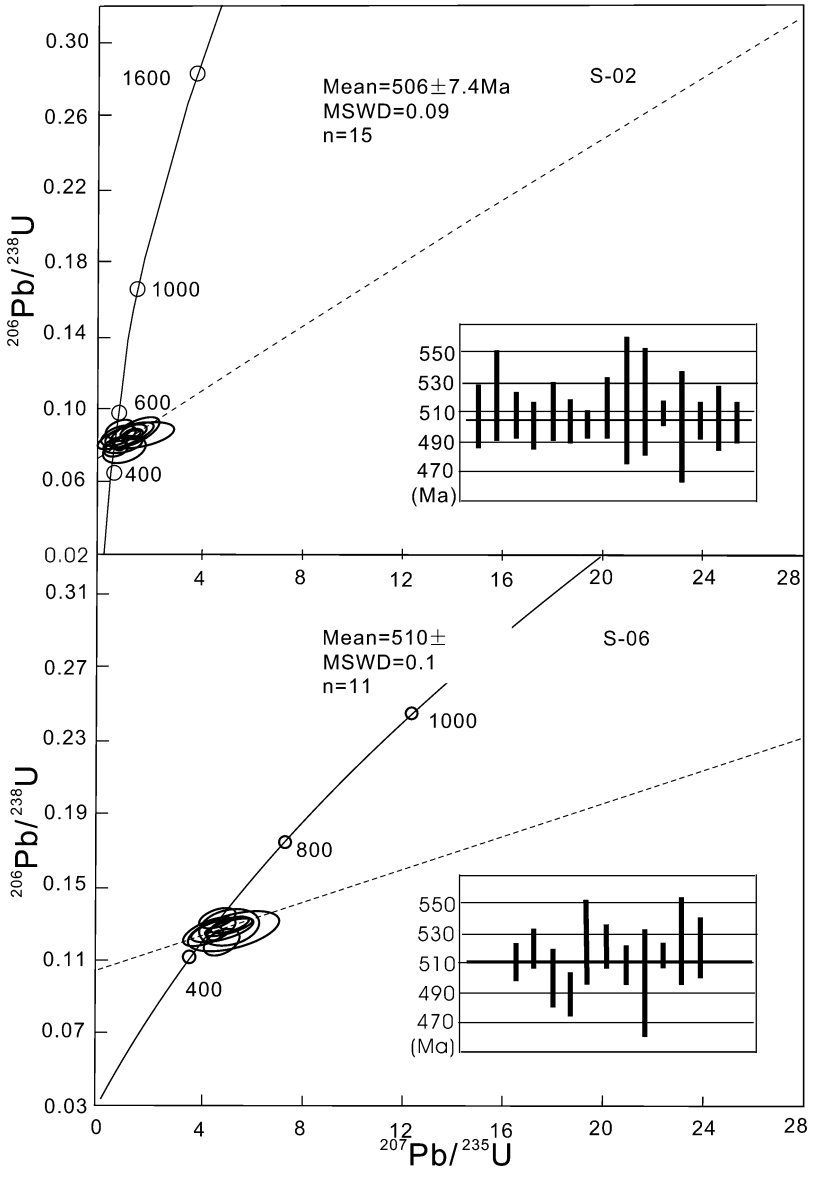

Figure 4. U–Pb ages of zircons in garnet amphibolites from the Songshugou ultramafic massif.

argue that the Songshugou ultramafic massif was emplaced during the Jinning orogeny at ~1.0 Ga (Li *et al.* 1991) and that there were major Proterozoic tectonic events in the North Qinling region (H.F. Zhang *et al.* 1998; Zhang *et al.* 2001). The Sm−Nd isochron age of 983 ± 140 Ma was obtained by using garnet, amphibole and whole rock from the garnet amphibolite in the contact metamorphic zone (Li *et al.* 1991). This age is consistent with a zircon U−Pb age (973 ± 35 Ma) for the amphibolite near the contact metamorphic zone (Liu *et al.* 2004). The zircon however, is magmatic in origin, and thus the U−Pb age represents the formation age of the protolith (Liu *et al.* 2004). Nonetheless, the large error (983 ± 140 Ma) of the

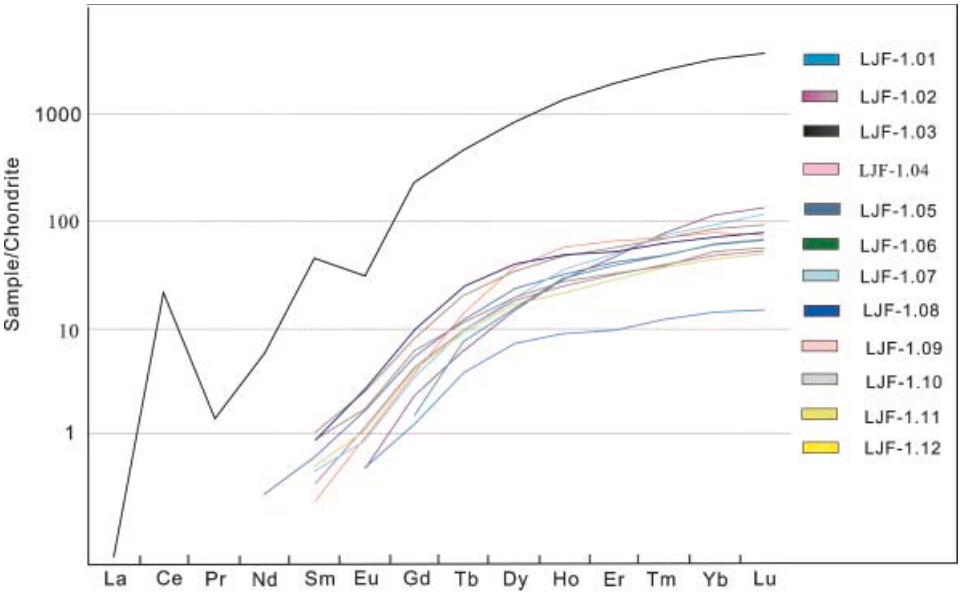

Figure 5. Trace element abundance patterns, normalized to chondrite for zircon from garnet amphibolite in the contact metamorphic zone. Normalization after Sun and McDonough (1989).

Sm−Nd isochron age implies that this age is not very reliable. One possible reason for the large error of the Sm−Nd isochron is that garnet was formed during the exhumation of the ultramafic massif, whereas amphibole might also have formed during the regional metamorphism before the contact metamorphism. Alternatively, relics of high-pressure granulite or garnet clinopyroxenite overprinted by the amphibolite facies in the contact metamorphic zone (Liu and Zhou 1994; Liu *et al.* 1995) imply that garnet was probably formed earlier than some of the amphibole. In addition, retrograde metamorphism may also have influenced the Sm−Nd system.

The distribution of the contact metamorphic zone is closely associated with the Songshugou massif, implying that it was formed during emplacement of the massif (Dong *et al.* 1997). Given that most of the zircon grains studied here are metamorphic in origin with low Th/U, the dating results of zircon represent the age of the emplacement. This is strongly supported by zircon trace element data.

One zircon grain (LJF-1.03) has distinctively high heavy REE contents with a negative Eu anomaly, indicating that this grain formed in the presence of plagioclase before garnet appeared. This zircon grain was likely formed at the early stage of the metamorphism induced by the intrusion of the ultramafic body. By contrast, all other zircon grains have consistent REE patterns, with low heavy REE contents and no Eu anomaly, similar to those of eclogitic zircon, suggesting that these grains formed after garnet appeared (Sun *et al.* 2002a). The U/Pb ages zircon grains with different REE patterns, however, are identical to each other within error (Table 1), indicating the emplacement of the ultramafic massif lasted for a very short period. Therefore, their ages (~510 Ma) represent the formation of garnet amphibolite, and the emplacement of the Songshugou massif into amphibolite of the Proterozoic Qinling Group. These ages, together with ultrahigh-pressure metamorphic rocks of the same age, indicate a major tectonic event occurred in the early Paleozoic

Table 2. Trace element concentrations for zircon from the garnet amphibolite in the contact metamorphic zone (all values are reported in ppm).

Element	LJF-1.01	LJF-1.02	LJF-1.03	LJF-1.04	LJF-1.05	LJF-1.06	LJF-1.07	LJF-1.08	LJF-1.09	LJF-1.10	LJF-1.11	LJF-1.12
Si29	153225	153225	153225	153225	153225	153225	153225	153225	153225	153225	153225	153225
P31	52.4	72.1	349.7	59.2	50.4	63.8	66.9	59.5	53.2	70.4	58.5	66.4
Ca42	<166	<160.43	<157.58	<192.46	<243.63	<168.23	<166.36	<157.47	<186.34	<179.96	576.76	<183.74
Sc45	201	222	237	219	232	264	236	252	233	255	217	225
Y89	23.7	69.6	3196	81.8	72.6	162	92.7	139	75.7	98.5	65.4	133
La139	<0.0154	<0.0141	0.025	0.0155	<0.020	<0.0191	<0.0170	<0.016	0.016	<0.0148	<0.0198	<0.0184
Ce140	0.031	0.346	19.6	0.15	0.041	0.129	0.365	0.319	0.403	0.177	0.302	0.505
Pr141	<0.0111	<0.0100	0.195	<0.0140	<0.016	<0.0103	<0.0111	<0.0168	<0.0154	<0.0135	<0.0151	<0.0154
Nd143	<0.084	<0.082	4.10	<0.071	0.17	<0.096	0.192	<0.093	<0.096	<0.106	<0.086	<0.103
Sm147	<0.062	0.075	10.5	<0.082	<0.083	0.052	0.138	0.199	0.246	0.102	0.113	0.238
Eu151	0.040	0.097	2.73	0.041	<0.034	0.078	0.141	0.22	0.146	0.073	0.093	0.218
Gd157	0.373	1.25	71.61	0.680	0.450	1.16	1.55	2.92	1.84	1.02	1.23	2.45
Tb159	0.219	0.538	26.91	0.343	0.416	0.781	0.664	1.398	0.651	0.509	0.522	1.172
Dy163	2.65	6.44	324.09	5.46	5.89	13.5	8.44	14.8	7.31	7.25	6.15	13.2
Ho165	0.735	2.01	120	2.39	2.27	4.88	2.7	4.1	2.237	2.94	1.80	4.00
Er166	2.34	7.48	493	11.48	9.28	16.16	9.98	12.9	7.94	12.16	6.92	13.91
Tm169	0.416	1.35	95.4	2.73	1.70	2.48	1.69	2.17	1.34	2.54	1.27	2.44
Yb173	3.41	11.6	843	27.8	14.6	18.7	15.3	17.8	12.6	22.9	10.7	21.0
Lu175	0.571	1.931	145	5.07	2.59	2.88	2.51	2.94	2.097	4.34	1.807	3.59
Pb208	0.293	0.59	17.7	0.322	1.08	0.373	0.984	0.953	0.654	0.107	0.18	0.165
Th232	0.0394	0.326	255	0.253	0.266	0.119	0.283	0.247	1.20	0.174	0.567	0.795
U238	4.37	10.4	211	6.20	3.41	16.0	11.3	21.8	13.04	7.38	8.74	16.3

All values are reported in ppm

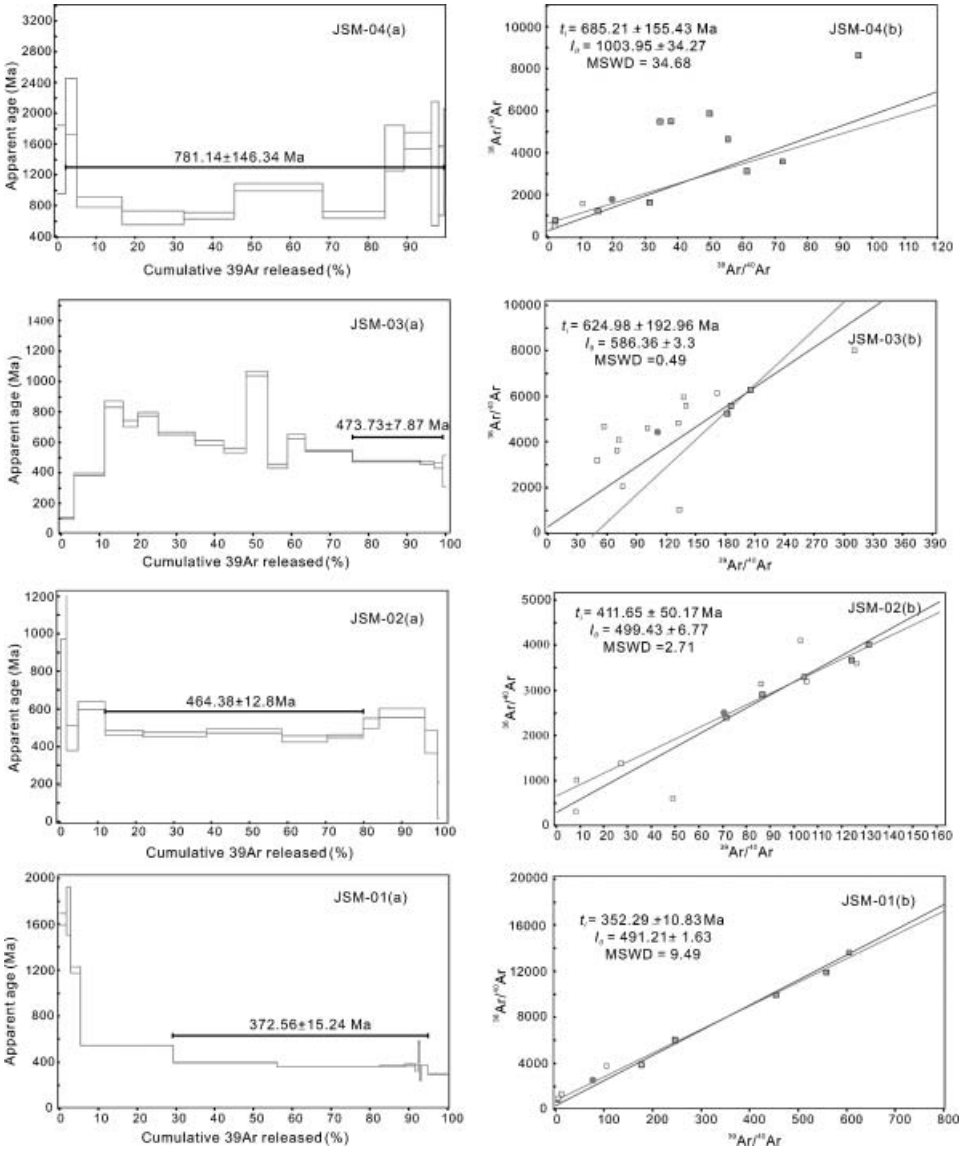

Figure 6. Diagrams of Ar–Ar age spectrum (a) and isochron (b) of amphibole from the garnet amphibolite and amphibolite in the contact metamorphic zone. (JSM-04 is amphibolite, others are garnet amphibolite). Available in colour online.

(~480−510 Ma) in the North Qinling region. This event was probably related to the closure of the North Qinling arc system (Xue *et al.* 1996; Sun *et al.* 2002b).

$^{40}Ar/^{39}Ar$ ages of amphibole from Songshugou garnet amphibolite contact metamorphic zone by laser stepwise heating increase from ~370 Ma for the inner garnet amphibolite sample to ~780 Ma for the amphibolite sample ~20 m away from the ultramafic massif. All those ages are younger than magmatic zircon U/Pb ages (~1.0 Ga) for amphibolite nearby (Liu *et al.* 2004), indicating that the K−Ar system of those samples has been disturbed during by regional metamorphism and/or during the emplacement of the Songshugou ultramafic massif. The age of sample

Table 3. Ar–Ar dating results of amphibole from garnet amphibolite in the contact metamorphic zone.

Step	Laser power	36Ar(a)	37Ar(ca)	38Ar(cl)	39Ar(k)	40Ar(r)	Age + 1σ (Ma)	40Ar(k)%	39Ar(k)%
	JSM-01, Hornblende from garnet amphibolite, laser stepwise heating.								
1	2.00 W	0.000071	0.000698	0.000002	0.000277	0.039094	1641 ± 50	65.14	1.84
2	2.50 W	0.000034	0.000338	0.000001	0.000151	0.022827	1714 ± 210	69.72	1.00
3	3.00 W	0.000032	0.002882	0.000008	0.000377	0.033941	1202 ± 30	78.27	2.50
4	4.00 W	0.000034	0.049181	0.000073	0.003596	0.120828	546 ± 2.2	92.20	23.90
5	4.50 W	0.000016	0.050227	0.000069	0.004034	0.094482	397 ± 1.5	95.09	26.80
6	5.60 W	0.000007	0.035553	0.000038	0.003989	0.083257	358 ± 1	97.49	26.50
7	5.90 W	0.000002	0.009572	0.000010	0.000969	0.020644	364 ± 8	97.01	6.44
8	6.20 W	0.000001	0.004068	0.000004	0.000404	0.008914	376.1 ± 7.7	97.81	2.69
9	6.50 W	0.000001	0.000730	0.000001	0.000107	0.002183	351 ± 29	92.38	0.71
10	6.80 W	0.000000	0.000295	0.000000	0.000069	0.002455	575.2 ± 6.1	99.98	0.46
11	7.20 W	0.000000	0.000309	0.000000	0.000047	0.000641	241.2 ± 4.4	99.96	0.31
12	8.00 W	0.000000	0.003133	0.000002	0.000258	0.005662	374.2 ± 1.7	99.97	1.72
13	10.00 W	0.000000	0.001296	0.000001	0.000772	0.013156	297.3 ± 1.5	99.96	5.13
	JSM-02, Hornblende from garnet amphibolite, laser stepwise heating.								
1	2.00 W	0.000003	0.000000	0.000000	0.000021	0.000052	46 ± 141	6.56	0.39
2	3.00 W	0.000009	0.001679	0.000000	0.000077	0.006648	1133 ± 159	71.00	1.47
3	3.50 W	0.000001	0.002236	0.000000	0.000152	0.004202	446 ± 66	90.76	2.89
4	4.20 W	0.000014	0.008270	0.000002	0.000381	0.015294	616 + 22	78.72	7.24
5	4.80 W	0.000007	0.014378	0.000002	0.000527	0.015559	473 ± 13	87.68	10.01
6	6.00 W	0.000008	0.025223	0.000003	0.000873	0.025157	462 ± 12	91.02	16.60
7	7.00 W	0.000012	0.027920	0.000006	0.001044	0.031557	483 ± 10	89.84	19.85
8	8.00 W	0.000005	0.019089	0.000003	0.000627	0.017086	440 ± 18	91.95	11.93
9	10.00 W	0.000004	0.014224	0.000003	0.000497	0.014065	456 ± 8	92.62	9.44
10	12.00 W	0.000003	0.007115	0.000002	0.000219	0.007286	524 ± 28	90.61	4.17
11	15.00 W	0.000006	0.018455	0.000007	0.000635	0.023602	577 ± 23	92.80	12.07
12	20.00 W	0.000001	0.004533	0.000001	0.000175	0.004576	425 ± 61	91.78	3.32
13	30.00 W	0.000001	0.000354	0.000000	0.000032	0.000202	112 ± 97	51.19	0.61

Table 3. (*Continued.*)

Step	Laser power	36Ar(a)	37Ar(ca)	38Ar(cl)	39Ar(k)	40Ar(r)	Age + 1σ (Ma)	40Ar(k)%	39Ar(k)%
	JSM-03, Hornblende from garnet amphibolite, laser stepwise heating.								
1	2.00 W	0.000006	0.000009	0.000000	0.000743	0.004153	101 ± 6	71.53	3.50
2	2.50 W	0.000022	0.000494	0.000002	0.001672	0.039107	390 ± 6	85.72	7.88
3	3.00 W	0.000021	0.006906	0.000010	0.001027	0.060193	850 ± 21	90.82	4.84
4	3.30 W	0.000011	0.007216	0.000010	0.000800	0.038233	723 ± 20	91.87	3.77
5	3.60 W	0.000016	0.011175	0.000013	0.001126	0.059576	786 ± 12	92.77	5.30
6	4.00 W	0.000020	0.026404	0.000031	0.002016	0.086373	660 ± 10	93.60	9.50
7	4.20 W	0.000011	0.022431	0.000028	0.001608	0.061062	596 ± 14	94.72	7.58
8	4.50 W	0.000009	0.016820	0.000020	0.001240	0.042691	548 ± 16	93.88	5.84
9	4.80 W	0.000021	0.015428	0.000023	0.001190	0.091543	1054 ± 15	93.68	5.61
10	5.00 W	0.000006	0.010989	0.000015	0.001079	0.029314	446 ± 13	94.36	5.09
11	5.30 W	0.000007	0.012053	0.000017	0.000993	0.040949	640 ± 16	95.04	4.68
12	6.00 W	0.000015	0.034814	0.000043	0.002576	0.088123	545 ± 5	95.19	12.14
13	8.00 W	0.000018	0.055854	0.000067	0.003772	0.110295	476 ± 3	95.29	17.77
14	10.00 W	0.000004	0.010890	0.000012	0.000748	0.021365	466 ± 9	94.69	3.52
15	15.00 W	0.000003	0.006408	0.000009	0.000489	0.013399	449 ± 18	94.37	2.31
16	20.00 W	0.000000	0.001825	0.000003	0.000142	0.003543	412 ± 102	96.29	0.67
	JSM-04, Hornblende from amphibolite, laser stepwise heating.								
1	2.50 W	0.000023	0.000535	0.000000	0.000044	0.005193	1397 ± 445	42.82	2.20
2	3.00 W	0.000026	0.001114	0.000002	0.000057	0.012634	2089 ± 363	61.83	2.87
3	3.50 W	0.000015	0.001639	0.000003	0.000233	0.014090	845 ± 68	75.86	11.69
4	4.00 W	0.000010	0.002609	0.000004	0.000317	0.013760	644 ± 89	82.10	15.89
5	4.50 W	0.000004	0.003856	0.000006	0.000260	0.011864	671 ± 39	91.76	13.04
6	5.20 W	0.000008	0.007698	0.000006	0.000451	0.035511	1038 ± 49	93.64	22.63
7	5.70 W	0.000005	0.026906	0.000025	0.000320	0.014890	682 ± 46	90.58	16.03
8	6.50 W	0.000003	0.012059	0.000003	0.000098	0.013534	1548 ± 293	94.64	4.93
9	8.00 W	0.000004	0.030208	0.000006	0.000140	0.021047	1644 + 106	94.61	7.00
10	9.00 W	0.000001	0.016676	0.000003	0.000035	0.003940	1345 ± 805	94.96	1.76
11	12.00 W	0.000000	0.032227	0.000001	0.000027	0.002325	1120 ± 449	96.57	1.34
12	15.00 W	0.000001	0.010807	0.000000	0.000012	0.001511	1426 ± 630	81.37	0.62

JSM-04 has a bigger error, and is older than emplacement ages of the ultramafic massif, indicating that its K−Ar system was not totally reset by the ultramafic massif. The amphibole $^{40}Ar/^{39}Ar$ ages of other samples are considerably younger than the emplacement ages of the ultramafic massif, suggesting a very slow cooling history of contact metamorphic zone after the ultramafic massif emplacement.

Previous authors proposed that the Songshugou massif formed through large-scale porous percolation flow of high-MgO melts probably related to the Rodinia superplume (~825 Ma) (Su *et al.* 2005) based on melt inclusions and an $^{40}Ar/^{39}Ar$ age of 848.2 ± 4.3 Ma for clinopyroxene megacrysts found in the ultramafic massif (Chen *et al.* 2002). The Rodinia superplume is represented by widely distributed mafic dikes of ~825 Ma in South China (Z.X. Li *et al.* 2003; W.X. Li *et al.* 2005; Li *et al.* 2005a). A recent study showed that the formation age of the Jinchuan ultramafic intrusion ranges from 812 ± 26 Ma to 827 ± 8 Ma, which is the same as the age of the Rodinia superplume within uncertainties. Based on geochemical characteristics of the Jinchuan ultramafic intrusions, it has been proposed that Jinchuan was also part of the Rodinia superplume (Li *et al.* 2005a). The $^{40}Ar/^{39}Ar$ age of 848.2 ± 4.3 Ma for clinopyroxene megacrysts from Songshugou is however, older than the age of the Rodinia superplume (825 Ma). Moreover, the closure temperature of a K−Ar system is lower than that of U−Pb in zircon. The peak metamorphic temperature in the contact metamorphic zone was ~800°C, which is much higher than the regional metamorphic temperature (Sun *et al.* 1997). Therefore, it is difficult to understand how the K−Ar system of the clinopyroxene megacrysts closed at such high temperatures. Further investigation is needed to understand the meaning of its $^{40}Ar/^{39}Ar$ age and to test whether the Songshugou massif was part of the Rodinia plume.

Implications on the evolution of Qinling orogenic belt

The Qinling orogenic belt was formed by the collision between the North and South China blocks (Zhang *et al.* 1995a, b; Zhang 1997; Meng and Zhang 1999; Sun *et al.* 2002a). Many authors agree that the Qinling orogen was built up through interplay of three major blocks, the North China Block (including the North Qinling), the South Qinling terrain, and the South China Block, with two sutures, the Shangdan and Mianlue (Zhang *et al.* 1995a; Meng and Zhang 2000; Zhang *et al.* 2004). The Shangdan suture resulted from the Middle Palaeozoic collision of the North China Block and the South Qinling (Meng and Zhang 1999). The Mianlue suture resulted from the Late Triassic collision of the South Qinling and the South China Block (Mattauer *et al.* 1985; Meng and Zhang 1999). The North Qinling, however, is different from the North China Block, but more or less similar to the South China Block, in terms of lead isotope (H.F. Zhang *et al.* 1998). This was used to argue that the North Qinling belong to the South China Block. Based on contrasting studies of Pb isotopic compositions between the North and South Qinling, it has been suggested that the Shangdan fault was not the main suture between the North and South China blocks in the Palaeozoic (Zhang 1997; H.F. Zhang *et al.* 1998). Others argued that these Pb isotope characteristics are also compatible with an arc setting of the North Qinling, considering that South China materials as well as isotopic signatures can be transported to the arc. Moreover, we are not clear when the North Qinling obtained its Pb isotope signature (Sun and Li 1998). Interestingly, zircon ages of ~960 to ~900 Ma for granitic gneisses in the North Qinling (Chen *et al.* 2006) imply its close association with the South China Block and the South Qinling

at ~900 Ma. Nonetheless, this cannot define the tectonic affinity of the North Qinling in the Palaeozoic.

Our results show that the Songshugou massif intruded into the Qinling group at ~510 Ma. There are two high- to ultrahigh-pressure metamorphic belts of similar ages discovered in the Qinling Group near the Songshugou massif (Liu and Zhou 1994; Yang *et al.* 2003). The south belt is only ~2 km away from the Songshugou ultramafic massif, whereas the north belt is ~20 km away. High-pressure mafic granulites from the south belt yielded LA-ICP-MS U−Pb zircon metamorphic ages of 485 ± 3.3 Ma (Chen *et al.* 2004), and diamond-bearing gneiss from the north belt yielded SHRIMP U–Pb zircon metamorphic ages of 502 ± 4.2 Ma (Yang *et al.* 2005). In addition, a SHRIMP zircon U−Pb age of 514 ± 1.3 Ma was obtained for the Fushui gabbroic complex (Su *et al.* 2004) near the Songshugou massif. One plausible interpretation is that the North Qinling separated from the South Qinling (South China Block) during the breakoff of Rodinia (Li *et al.* 1999), which then merged with, and became an active margin of, the North China Block. The nature of the event at ~500 Ma is still not very clear. It probably represents a collision between a microcontinent or island and the North Qinling (North China Block) in a southwest Pacific-type plate boundary.

The youngest $^{40}Ar/^{39}Ar$ age is about 130 Myr younger than the emplacement age of the Songshugou ultramafic body (~510 Ma). This young age is not likely to be due to re-setting of the garnet amphibolite during a late stage regional tectonothermal event, because $^{40}Ar/^{39}Ar$ age of amphiboles in the contact zone increases from the ultramafic massif outward (~370 to ~780 Ma), indicating close association with the massif. Therefore, the Songshugou ultramafic massif ascended and cooled at a very slow rate. A previous study indicates that the metamorphic peak temperature was ~800 °C (Sun *et al.* 1997). This corresponds to a cooling rate of 2.3°C/Myr, assuming the closure temperature of the K−Ar system is 500°C. Such a slow cooling rate suggested that either there was very limited uplift and consequent denudation between 550 and 370 Ma, or the Songshugou ultramafic massif was preserved at temperatures above the closure temperature of the K−Ar system for a long time and then was emplaced into the Qinling Group during regional tectonic events. The former is consistent with previous results (Sun and Yu 1991).

It is generally accepted that the ocean between the South and North China blocks closed along the Shang-Dan fault in the Palaeozoic (Meng and Zhang 1999), based on studies on geochronology, petrology, and field observations. Convergence of the two blocks did not result in the final continent collision and subsequent mountain-building, such that there was no obvious uplift in the Qinling orogenic belt associated with the Palaeozoic suturing (Sun and Yu 1991).

Conclusions

Geochronology analyses of garnet amphibolites in the contact-metamorphic zone indicate that the Songshugou ultramafic massif was emplaced at ~510 Ma, rather than 1000 Ma. Therefore, the Songshugou ultramafic massif did not result from the Jinning orogeny. Instead, it was emplaced into the Proterozoic Qinling Group during the Palaeozoic. It cannot be used to support major geological events in the Qinling region during the Jinning period. Our new data for the Songshugou ultramafic massif, together with ultrahigh-pressure metamorphic rocks of the same age, indicate that a major tectonic event occurred in the early Palaeozoic

(~480−510 Ma) in the North Qinling region, which was probably associated with closure of the North Qinling arc system.

Acknowledgements

This research was financially supported by MOST (2006CB403505) (No. 40525010) and the CAS/SAFEA International Partnership Programme for Creative Research Teams to WDS. We thank Y.M. Sun, Y. Yang, Y.L. Liu, X. Ding and B. Zhou for constructive discussion. Thanks also to X.M. Liu and J.Q. Wang for laser ablation ICP-MS analyses and H.P. Li for field assistance. LT was supported by a GIG-CAS starting project (No. 0807011001). This is contribution No. IS-1012 from GIGCAS.

References

An, S., Wang, D., and Hu, N., 1981, Geological characteristics and genesis of ultramafities in Songshugou area, Shangnan, Shaanxi Province: Journal of Xi'an College of Geology, v. 2, p. 9–12 (in Chinese with English abstract).

Andersen, T., 2002, Correction of common lead in U–Pb analyses that do not report 204Pb: Chemical Geology, v. 192, p. 59–79.

Black, L.P., 2003, TEMORA 1: A new zircon standard for Phanerozoic U–Pb geochronology: Chemical Geology, v. 200, p. 155–170.

Chen, D.L., Liu, L., Sun, Y., Zhang, A.D., Liu, X.M., and Luo, J.H., 2004, LA-ICP-MS zircon U–Pb dating for high-pressure basic granulite from North Qinling and its geological significance: Chinese Science Bulletin, v. 49, p. 2296–2304.

Chen, D.L., Liu, L., Zhou, D.W., Luo, J.H., and Sang, Q.H., 2002, Genesis and $^{40}Ar/^{39}Ar$ dating of clinopyroxene megacrysts (Andersen 2002) in ultramafic terrain from Songshugou, eastern Qinling Mountain and its geological implication: Acta Petrologica Sinica, v. 18, p. 355–362 (in Chinese with English abstract).

Chen, Z.H., Lu, S.N., Li, H.K., Li, H.M., Xiang, Z.Q., Zhou, H.Y., and Song, B., 2006, Constraining the role of the Qinling orogen in the assembly and break-up of Rodinia: Tectonic implications for Neoproterozoic granite occurrences: Journal of Asian Earth Sciences, v. 28, p. 99–115.

Dong, Y., Zhou, D., and Zhang, G., 1997, The emplacement mechanism and tectonic evolution of ultramafities in Songshugou area, eastern Qinling: Scientia Geological Sinica, v. 32, p. 173–188.

Gao, C.L., 1990, Geochemical Characteistics of Mafic-ultramafic Rocks from Three Types of Structural Setting in Eastern Qinling: Wuhan, China University of Geoscences Press, p. 106–127.

Gilder, S., and Courtillot, V., 1997, Timing of the north–south China collision from new middle to late Mesozoic paleomagnetic data from the north China block: Journal of Geophysical Research-Solid Earth, v. 102, p. 17713–17727.

Güenther, D., Frischknecht, R., Heinrich, C.A., and Kahlert, H.J., 1997, Capabilities of an Argon Fluoride 193 nm excimer laser for laser ablation inductively coupled plasma mass spectrometry microanalysis of geological materials: Journal of Analytical Atomic Spectrometry, v. 12, p. 939–944.

Huang, Y., 1984, The aureoles of the Songshugou Alpine-type Massif: Geochimica et Cosmochimica Acta, v. 3, p. 206–215.

Koppers, A.P., 2002, ArArCALCF software for 40Ar/39Ar age calculations: Computers & Geosciences, v. 28, p. 605–619.

Lerch, M., 1993, Early Paleozoic tectonic evolution of the Qinling Orogenic Belt in the Heihe area, Central China. Mainz, p. 98 (unpublished data).

Lerch, M.F., Xue, F., Kroner, A., Zhang, G.W., and Tod, W., 1995, Middle Silurian – Early Devonian magmatic arc in the Qinling Mountains of Central China: Journal of Geology, v. 103, p. 437–449.

Li, S., Chen, Y., Zhang, G., and Zhang, Z., 1991, A 1Ga B. P. Alpine peridotite body emplaced into the Qinling Group: evidence for the existence of the late Proterozoic plate tectonics in the north Qinling area: Geological Review, v. 37, p. 235–242.

Li, Z.X., Li, X.H., Kinny, P.D., and Wang, J., 1999, The breakup of Rodinia: did it start with a mantle plume beneath South China?: Earth and Planetary Science Letters, v. 173, p. 171–181.

Li, Z.X., Li, X.H., Kinny, P.D., Wang, J., Zhang, S., and Zhou, H., 2003, Geochronology of Neoproterozoic syn-rift magmatism in the Yangtze Craton, south China and correlations with other continents: evidence for a mantle superplume that broke up Rodinia: Precambrian Research, v. 22, p. 85–109.

Li, W.X., Li, X.H., and Li, Z.X., 2005, Neoproterozoic bimodal magmatism in the Cathaysia Block of South China and its tectonic significance: Precambrian Research, v. 136, p. 51–66.

Li, X.H., Qi, C.S., Liu, Y., Liang, X.R., Tu, X.L., Xie, L.W., and Yang, Y.H., 2005a, Petrogenesis of the Neoproterozoic bimodal volcanic rocks along the western margin of the Yangtze Block: New constraints from Hf isotopes and Fe/Mn ratios: Chinese Science Bulletin, v. 50, p. 2481–2486.

Li, X.H., Su, L., Chung, S.L., Li, Z.X., Liu, Y., Song, B., and Liu, D.Y., 2005b, Formation of the Jinchuan ultramafic intrusion and the world's third largest Ni–Cu sulfide deposit: Associated with the similar to 825 Ma south China mantle plume?: Geochemistry Geophysics Geosystems, v. 6, p. Q11004.

Liu, L., Cheng, D., Zhang, A., Zhang, C., Yuan, H., and Luo, J., 2004, Geochemical Characteristics and LA-ICP-MS Zircon U–Pb dating of Amphibolites in the Songshugou Ophiolite in the Eastern Qinling: Acta Geologica Sinica, v. 78, p. 137–145.

Liu, X.M., Gao, S., Yuan, H.L., Bodo, H., Deltef, G., Cheng, L., and Hu, S.H., 2002, Analysis of 42 major and trace element in glass standard reference material by 193nm LA-ICPMS: Acta Petrologica Sinica, v. 18, p. 408–418.

Liu, J.F., and Sun, Y., 2005, New data on the 'hot' emplacement age of ultramafic rocks from the Songshugou area in the Eastern Qinling: Geological Review, v. 51, p. 189–192.

Liu, L., and Zhou, D.W., 1994, Discovery and study of high pressure basic granulites in Songshugou area of Shangdan, East Qinling: Chinese Science Bulletin, v. 39, p. 1599–1601.

Liu, L., Zhou, D., Dong, Y., Zhang, H., Liu, Y., and Zhang, Z., 1995, High pressure metabasites and their retrograde metamorphic PTt path from Songshugou area, eastern Qinling Mountain: Acta Petrologica sinica, v. 11, p. 127–136.

Mattauer, M., Matte, P., Malavieille, J., Tapponnier, P., Maluski, H., and Xu, Z.Q., 1985, Tectonics of the Qinling Belt: build-up and evolution of eastern Asia: Nature, v. 317, p. 496–500.

Meng, Q.R., and Zhang, G.W., 1999, Timing of collision of the North and South China blocks: Controversy and reconciliation: Geology, v. 27, p. 123–126.

———, 2000, Geologic framework and tectonic evolution of the Qinling Orogen, central China: Tectonophysics, v. 323, p. 183–196.

Northwest Metallurgy 713 Team, 1961, The geological map of Shangnan County (1: 200000).

Onstotta, T.C., Phillipsa, D., and Pringle-Goodella, L., 1991, Laser microprobe measurement of chlorine and argon zonation in biotite: Chemical Geology, v. 90, p. 145–168.

Pearce, N., Perkins, W., and Westgate, J., 1997, A compilation of new and published major and trace element data for NIST SRM 610 and NIST SRM 612 galss reference materials: Geostandards Newslett, v. 21, p. 115–144.

Pei, X., Zhang, W., and Wang, Q., 1996, Geological and Geochimical characteristics and their tectonic enviroment of Songshugou ophiolite in the north Qinling: Beijing, Geological Pulishing House, p. 49–52.

Qiu, H.N., and Wijbrans, J.R., 2006, Paleozoic ages and excess 40Ar in garnets from the Bixiling eclogite in Dabieshan, China: New insights from 40Ar/39Ar dating by stepwise crushing: Geochimica et Cosmochimica Acta, v. 70, p. 2354–2370.

Su, L., 2004, Studies of Neoproterozoic mafic and ultramafic intrusions in western-central China and their constraints on breakup of Rodinia Supercontinent [PhD thesis]: Xi'an, Northwest University, p. 67–96.

Su, L., Song, S., Song, B., Zhou, D., and Hao, J., 2004, SHRIMP zircon U–Pb ages of garnet pyroxenite and Fushui Gabbroic coplex in Songshugou region and constraints on tectonic evolution of Qinling Orogenic Belt: Chinese Science Bulletin, v. 49, p. 1209–1211.

Su, L., Song, S.G., and Zhou, D.W., 2005, Petrogenesis of Songshugou dunite body in the Qinling orogenic belt,Central China: Constraints from geochemistry and melt inclusions: Science in China Series D Earth Sciences, v. 48, p. 1146–1157.

Sun, W.D., and Li, S.G., 1998, Pb isotopes of granitoids suggest Devonian accretion of Yangtze (South China) craton to North China craton: Comment: Geology, v. 26, p. 859–860.

Sun, W., Li, S.G., Chen, Y.D., and Li, Y.J., 2002a, Timing of synorogenic granitoids in the South Qinling, central China: Constraints on the evolution of the Qinling–Dabie orogenic belt: Journal of Geology, v. 110, p. 457–468.

Sun, W., Li, S., Sun, Y., Zhang, G., and Li, Q., 2002b, Mid-paleozoic collision in the north Qinling: Sm–Pb, Rb–Sr, and 40Ar/39Ar ages and their tectonic implications: Journal of Asian Earth Sciences, v. 21, p. 69–76.

Sun, Y., and Yu, Z.P., 1991, A discussion on an ancient ocean and caledonian orogeny in the east Qinling, *in* Ye, L.J., Qian, L.X., and Zhang, G.W., eds., Collection in a Selection of Papers Presented at the Conference on the Qinling Orogenic Belt: Xi'an, Northwest University Press, p. 167–173.

Sun, W., Zheng, Y., Li, S., Sun, Y., and Zhang, G., 1997, An oxygen isotope study of contact metamorpjic rocks from Songshugou in North Qinling: Acta Petrologica Sinica, v. 13, p. 162–167.

Wang, X., Liou, J., and Mao, H., 1991, Coesite-bearing ecologites from the Dabie Mountains in central China: Geology, v. 17, p. 1085–1088.

Wang, X., Xu, C., Shi, R., and Chen, S., 2005, The Songshugou rock body from Qinling-an example of ultramafic cumulate undergone amphibolitic phases metamorphism: Acta Geologica Sinica, v. 79, p. 174–189.

Wang, H., Xu, C., and Zhou, Z., 1982, Tectonic evlution of continental margin of paleo-ocean in East Qinling: Acta Geologic Sinica, v. 3, p. 270–279 (in Chinese with English abstract).

Wiedenbeck, M., Alle, P., and Corfu, F., 1995, Three natural zircon standards for U–Th–Pb, Lu–Hf, trace element and REE analyses: Geostandards Newslett, v. 19, p. 1–23.

Xu, Z., Lu, Y., Tang, Y., and Zhang, Z., 1988, Formation of composite chain mountains Easter Qinling: Beijing, China Environmental Science Press, p. 655–724.

Xue, F., Lerch, M., Kroner, A., and Reischmann, T., 1996, Tectonic evlution of the east Qinling mountains, China, in the Palaeozoic: A review and new tectonic model: Tectonophysics, v. 253, p. 271–284.

Yang, J.S., Liu, F.L., Wu, C.L., Xu, Z.Q., Shi, R.D., Chen, S.Y., Deloule, E., and Wooden, J.L., 2005, Two ultrahigh-pressure metamorphic events recognized in the Central Orogenic Belt of China: Evidence from the U–Pb dating of coesite-bearing zircons: International Geology Review, v. 47, p. 327–343.

Yang, J.S., Xu, Z.Q., Dobrzhinetskaya, L.F., Green, H.W., Pei, X.Z., Shi, R.D., Wu, C.L., Wooden, J.L., Zhang, J.X., Wan, Y.S., and Li, H.B., 2003, Discovery of metamorphic diamonds in central China: an indication of a $>$ 4000-km-long zone of deep subduction resulting from multiple continental collisions: Terra Nova, v. 15, p. 370–379.

Yuan, H., Wu, F., Gao, S., Liu, X., Xu, P., and Sun, D., 2003, Determination of U–Pb age and rare earth element concentrations of zircon from Cenozoic intrusions in northeastern China by laser ablation ICP-MS: Chinese Science Bulletin, v. 48, p. 1511–1520.

Zhang, Z., 1993, The genetic classification of Songshugou ultramafic rocks in North Qinling mountains: Contributions to Geology and Mineral Resources Research, v. 8, p. 48–61.

Zhang, K.J., 1997, North and South China collision along the eastern and southern North China margins: Tectonophysics, v. 270, p. 145–156.

Zhang, G.W., Dong, Y.P., Lai, S.C., Guo, A.L., Meng, Q.R., Liu, S.F., Cheng, S.Y., Yao, A.P., Zhang, Z.Q., Pei, X.Z., and Li, S.Z., 2004, Mianlue tectonic zone and Mianlue suture zone on southern margin of Qinling–Dabie orogenic belt: Science in China Series D-Earth Sciences, v. 47, p. 300–316.

Zhang, H.F., Gao, S., Zhang, B.R., Luo, T.C., and Lin, W.L., 1998, Pb isotopes of granitoids suggest Devonian accretion of Yangtze (South China) craton to North China craton: a Reply: Geology, v. 26, p. 860–861.

Zhang, B., Han, Y., Xu, J., and Ouyang, J., 1998, Geochemical evidence for north Qinling being part of Yangtze plate prior to the Neoproterozoic: Geological Journal of China's Universities, v. 4, p. 369–382.

Zhang, G.W., Meng, Q.G., and Lai, S.C., 1995a, Tectonics and Structure of Qinling Orogenic Belt: Science in China Series B-Chemistry Life Sciences & Earth Sciences, v. 38, p. 1379–1394.

Zhang, G.W., Xiang, L.W., and Meng, Q.G., 1995b, The Qinling Orogen and Intracontinental Orogen Mechanisms: Episodes, v. 18, p. 36–39.

Zhang, G.W., Yu, Z.P., Sun, Y., Cheng, S.Y., Li, T.H., Xue, F., and Zhang, C.L., 1989, The major suture zone of the Qinling orogenic belt: Journal of Southeast Asian Earth Science, v. 3, p. 1–13.

Zhang, G., Zhang, B., Yuan, X., and Xiao, Q., 2001, Qinling orogenic belt and continetal dynamics: Beijing, Science Press, p. 655–724.

Zhang, G., Zhou, D., Yu, Z., Gu, A., Cheng, X., Li, T., Zhang, C., and Xue, F., 1991, Characteristics of the lithopheric composition, structure and evolution of the Qinling orogenic belt, *in* Ye, L., Qian, L., and Zhang, G., eds., A selection of Papers Presented at the conference on the Qinling Orogenic Belt: Xi'an, Northwest University Press, p. 121–138.

Zhou, D., Zhang, Z., Dong, Y., and Liu, L., 1995, Geological and geochemical characteristics on Proterozoic Songshugou ophiolite piece from shangnan country, Qinling: Acta Petrologica Sinica, v. 11, p. 154–164 (in Chinese with English abstract).